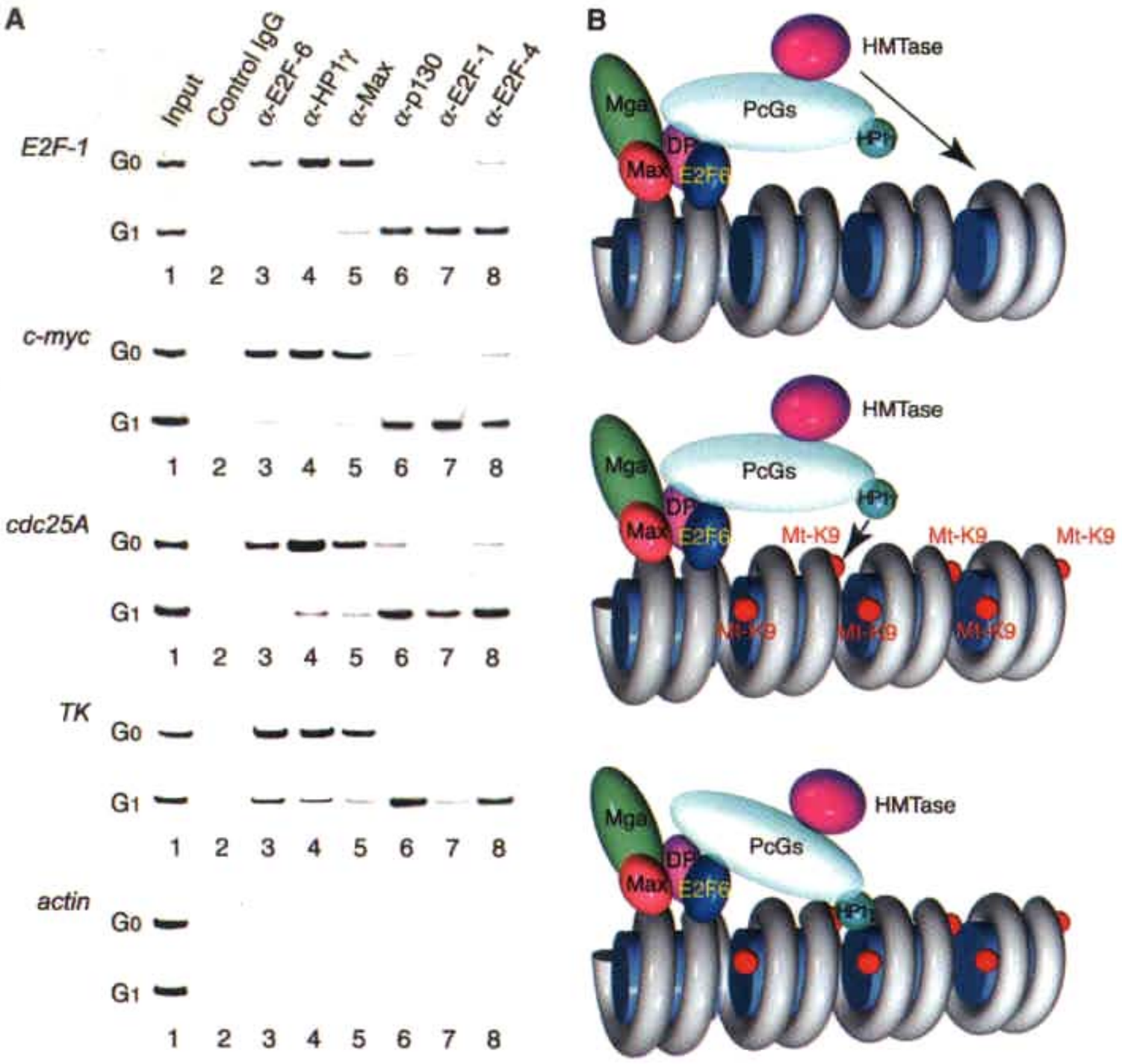

Fig. 5. (**A**) Binding of E2F6.com-1 to the target promoters in vivo. Chromatin immunoprecipitation was performed from G_0 (top) and G_1 (bottom) cells with the indicated antibodies. The presence of target genes in the immunoprecipitates was detected by PCR with primers that amplify *E2F-1*, *cdc25A*, *c-myc*, and *TK* promoters as well as β-*actin*-coding region. (**B**) Model of repression by E2F6.com-1 via formation of transcriptionally inactive chromatin.

As illustrated in Fig. 5B, E2F6.com-1 could be recruited on E2F- and Myc-responsive genes via sequence-specific DNA binding domains in the complex (top), and it could methylate proximate nucleosomes (middle) and load HP1γ and PcG proteins (bottom). This recruitment could form a "platform" that is required for nucleating PcG proteins and which thus contribute to the propagation of inactive chromatin, leading to entire repressed regions.

It is intriguing that E2F6.com-1 is present in HeLa cells that cannot enter the quiescent stage, even though it does not occupy target genes. Revealing the details of these processes would provide further insights into mechanisms whereby normal cells can enter quiescent stage, whereas malignant tumor cells cannot.

Note added in proof: In contrast to our data, Takahashi *et al. (22)* reported that p130 and E2F4 occupy the target promoters in G_0 and early G_1 stages. We believe that this discrepancy could be due to different cell types and conditions for G_0 induction. Takahashi *et al.* used T98G human glioblastoma cells, whereas we used human BJ-1 fibroblasts. Moreover, they arrested the cell cycle by serum starvation, whereas we first arrested the cycle by contact inhibition, then by serum starvation.

References and Notes

1. N. Dyson, *Genes Dev.* **12**, 2245 (1998).
2. H. Muller, K. Helin, *Biochim. Biophys. Acta* **1470**, M1 (2000).
3. C. Grandori, S. M. Cowley, L. P. James, R. N. Eisenman, *Annu. Rev. Cell. Dev. Biol.* **16**, 653 (2000).
4. M. M. Lipinski, T. Jacks, *Oncogene* **18**, 7873 (1999).
5. X. Grana, J. Garriga, X. Mayol, *Oncogene* **17**, 3365 (1998).
6. M. Malumbres, M. Barbacid, *Nature Rev. Cancer* **1**, 222 (2001).
7. S. Gaubatz, J. G. Wood, D. M. Livingston, *Proc. Natl. Acad. Sci. U.S.A.* **95**, 9190 (1998).
8. P. Cartwright, H. Muller, C. Wagener, K. Holm, K. Helin, *Oncogene* **17**, 611 (1998).
9. J. M. Trimarchi *et al.*, *Proc. Natl. Acad. Sci. U.S.A.* **95**, 2850 (1998).
10. Materials and methods are available as supporting online material.
11. H. Ogawa, Y. Nakatani, unpublished observations.
12. P. J. Hurlin, E. Steingrimsson, N. G. Copeland, N. A. Jenkins, R. N. Eisenman, *EMBO J.* **18**, 7019 (1999).
13. U. Technau, *Bioessays* **23**, 788 (2001).
14. GenBank accession number AY083210.
15. M. Tachibana, K. Sugimoto, T. Fukushima, Y. Shinkai, *J. Biol. Chem.* **276**, 25309 (2001).
16. S. E. Brown, R. D. Campbell, C. M. Sanderson, *Mamm. Genome* **12**, 916 (2001).
17. M. Lachner, D. O'Carroll, S. Rea, K. Mechtler, T. Jenuwein, *Nature* **410**, 116 (2001).
18. A. J. Bannister *et al.*, *Nature* **410**, 120 (2001).
19. D. O. Jones, I. G. Cowell, P. B. Singh, *Bioessays* **22**, 124 (2000).
20. J. L. Kalenik, D. Chen, M. E. Bradley, S. J. Chen, T. C. Lee, *Nucleic Acids Res.* **25**, 843 (1997).
21. J. M. Trimarchi, B. Fairchild, J. Wen, J. A. Lees, *Proc. Natl. Acad. Sci. U.S.A.* **98**, 1519 (2001).
22. Y. Takahashi *et al.*, *Genes Dev.* **14**, 804 (2000).

23. We would like to thank colleagues in the Nakatani and Livingston labs for discussions and reagents; B. Eisenman, M. van Lohuizen, and G. Cavalli for useful comments; P. Hurlin, J. Lees, and M. Vidal for antibodies; members of the DFCI Molecular Core Facility and Taplin Biological Mass Spectrometry Facility for their assistance. This work was supported, in part, by grants from Claudia Adams Barr Program (Y.N.), Human Frontier Science Program (Y.N.) and the National Cancer Institute (D.M.L.). H.O. is supported by a fellowship from Japan Science and Technology.

Supporting Online Material

(www.sciencemag.org/cgi/content/full/296/5510/1132/DC1)
Materials and Methods
References

15 January 2002; accepted 19 March 2002

Autosomal Dominant Mutations Affecting X Inactivation Choice in the Mouse

Ivona Percec,[1,2] Robert M. Plenge,[2]* Joseph H. Nadeau,[2] Marisa S. Bartolomei,[1]† Huntington F. Willard[2,3]†

X chromosome inactivation is the silencing mechanism eutherian mammals use to equalize the expression of X-linked genes between males and females early in embryonic development. In the mouse, genetic control of inactivation requires elements within the X inactivation center (*Xic*) on the X chromosome that influence the choice of which X chromosome is to be inactivated in individual cells. It has long been posited that unidentified autosomal factors are essential to the process. We have used chemical mutagenesis in the mouse to identify specific factors involved in X inactivation and report two genetically distinct autosomal mutations with dominant effects on X chromosome choice early in embryogenesis.

During early preimplantation development, female cells have two active X chromosomes. As these cells begin to differentiate, they undergo X chromosome inactivation, the epigenetic process that results in the stable silencing of a majority of genes on one X

chromosome (*1–4*). Historically, control of inactivation has been attributed to a genetically defined region on the X chromosome known as the X inactivation center (*Xic*); three elements have been mapped to *Xic* that play a role in the mechanism of inactivation. A key component is the *Xist* gene and its product (*5*), a large untranslated RNA that coats the inactive X chromosome (X_i). It is transcribed from the X_i, whereas it is repressed on the active X (X_a). *Xist* is required in cis for initiation and propagation of silencing (*2*, *3*, *6*). Its antisense counterpart, *Tsix* (*7*), is transcribed exclusively from X_a and appears to repress *Xist* before initiation of X inactivation, thereby maintaining two active X chromosomes (*7*, *8*). Once silenced, the inactive X maintains its state by a variety of epigenetic regulatory mechanisms, including modification of both classic and variant histones, methylation of X_i DNA, and late replication timing (*2–4*).

The most elusive component of the X inactivation pathway remains the initial choice between the two X chromosomes, the earliest step in the process. In the mouse, choice is under the control of the X-controlling element (*Xce*), a third locus within the *Xic* (*9–12*). Three *Xce* alleles (Xce^a, Xce^b, and Xce^c) have been described (*13*, *14*), and mutation studies of the *Xist* and *Tsix* genes suggest that they also play a role in choice (*2*, *3*). Further, *DXPas34*, a region downstream from the *Tsix* promoter, is hypermethylated on *Xce* alleles that are more likely to remain active (*15*). It has long been hypothesized that multiple trans-acting autosomal factors interact with cis-acting elements in the *Xic* to determine X chromosome choice (*16–19*). Recent identification of CTCF-binding sites within *Tsix* suggests that the general transcriptional regulator CTCF may behave as one such factor (*20*), although there is no genetic evidence that CTCF influences X inactivation (*21*). To identify specific trans-acting elements that act on the choice process, we conducted a phenotype-driven genetic screen involving chemical mutagenesis in the mouse.

The screen took advantage of a quantitative mouse model of choice in which the effect of different *Xce* alleles is used as a baseline measure of the X inactivation pattern (*22*). Nonrandom choice occurs when a "strong" *Xce* allele (one that is more likely to be on the active X, such as the Xce^c allele derived from *Mus musculus castaneus* mice) is inherited in combination with a "weak" allele (one that is less likely to be on the active X, such as Xce^a or Xce^b derived from *Mus musculus domesticus* mice). In these heterozygous animals, 25 to 30% of cells choose the X bearing the weaker *Xce* allele as the X_a, instead of the 50% expected for a completely random process (*10–14*, *22*). The use of $Xce^{a/c}$ and $Xce^{b/c}$ heterozygotes in the genetic screen facilitated recovery of mutations disrupting general aspects of X chromosome choice as well as those specifically involved in *Xce* allelic discrimination.

The X inactivation phenotype was first established in two unmutagenized control populations of $Xce^{a/c}$ and $Xce^{b/c}$ heterozygotes to provide a basis for screening the mutagenized populations (*22*, *23*). We then screened 84 $Xce^{a/c}$ and 252 $Xce^{b/c}$ G_1 female progeny of males treated with *N*-ethyl-*N*-nitrosourea (ENU) (Fig. 1, A and D) (*23*, *24*). We considered any G_1 animals with X inactivation patterns greater than two standard deviations from the mean of the control populations candidates for X inactivation mutants. To avoid recovering animals in which deleterious X-linked mutations unrelated to the X inactivation choice pathway caused highly skewed X inactivation patterns secondary to differential cell survival (*25*), we concentrated on animals that preferentially maintained the mutagenized X chromosome as the X_a. To determine the heritability of the putative mutations, we progeny tested G_1 females fulfilling the candidate mutant criteria.

Two G_1 females, 24.21 and 1.19 (*26*), transmitted the altered X inactivation pattern to their female offspring and were investigated further. Both pedigrees segregated the mutant X inactivation pattern through at least the seventh generation and demonstrated dominant inheritance patterns (Fig. 1, B, C, E, and F). In both pedigrees, carrier females (*26*) displayed X inactivation patterns significantly different from those predicted by their respective *Xce* genotypes, as the X chromosome bearing the strong *Xce* allele was the X_i in a significantly higher proportion of cells than expected (*22*). Phenotyping several generations of outcrossed control animals confirmed that the aberrant X inactivation pat-

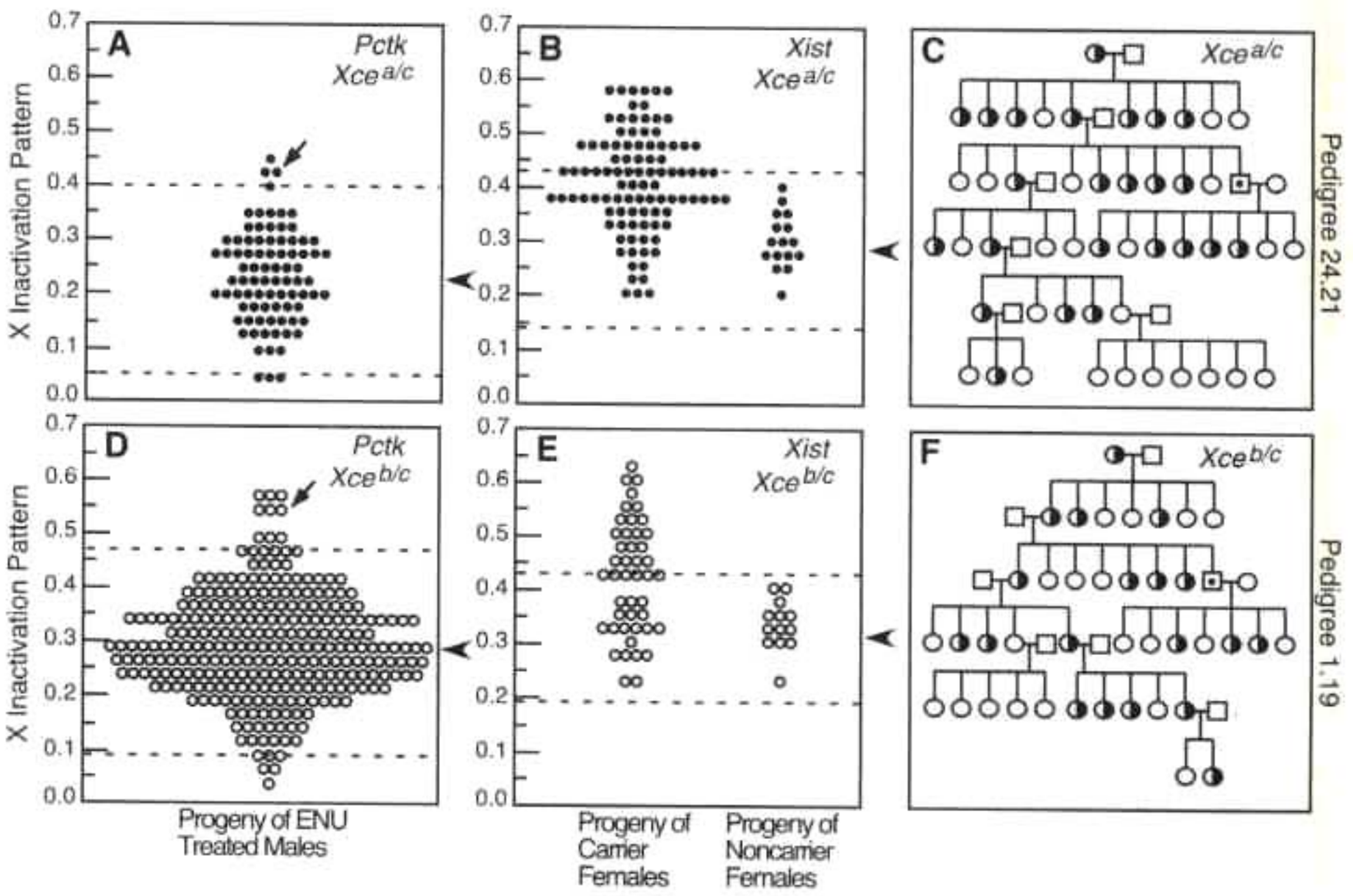

Fig. 1. Mutagenesis screen and progeny tests of two mutants: 24.21 and 1.19. Distribution of the X inactivation pattern in 84 G_1 $Xce^{a/c}$ (closed circles) (**A**) and 252 G_1 $Xce^{b/c}$ (open circles) (**D**) female progeny of ENU-treated males. Females 24.21 and 1.19 are designated by diagonal arrows in (A) and (D), respectively. The X inactivation pattern reflects the proportion of *M. musculus domesticus* allele transcription relative to total RNA levels of both *M. musculus domesticus* and *M. musculus castaneus* alleles (*22*, *24*). Progeny tests of the $Xce^{a/c}$ G_1 female 24.21 (**B**) and the $Xce^{b/c}$ G_1 female 1.19 (**E**) demonstrate dominant transmission of each mutant phenotype through the seventh generation. Unaffected females from each pedigree generated only unaffected female progeny [right (B) and (E)]. In (A), (B), (D), and (E), the horizontal arrowhead represents the mean X inactivation pattern, and the dashed lines represent the 2 SD demarcation of matched control (unmutagenized) populations (*22*, *26*). Representative branches of the 24.21 (**C**) and 1.19 (**F**) pedigrees demonstrate dominant segregation of each mutation through affected females (half-filled circles) and through carrier males with a wild-type X chromosome (squares with a dot) but not through unaffected females (open circles). Affected females are defined by phenotypes that are at least 2 SD greater than the mean of controls. Carrier status was confirmed by transmission of the affected phenotype to at least two female offspring (*26*).

[1]Howard Hughes Medical Institute and Department of Cell and Developmental Biology, University of Pennsylvania School of Medicine, Philadelphia, PA 19104, USA. [2]Department of Genetics, Case Western Reserve University School of Medicine, Cleveland, OH 44106, USA. [3]Research Institute and Center for Human Genetics, University Hospitals of Cleveland, Cleveland, OH 44106, USA.

*Present address: Department of Medicine, University of California, San Francisco, CA 94143, USA.

†To whom correspondence should be addressed. E-mail: bartolom@mail.med.upenn.edu (M.S.B.) and willard@uhri.org (H.F.W.).

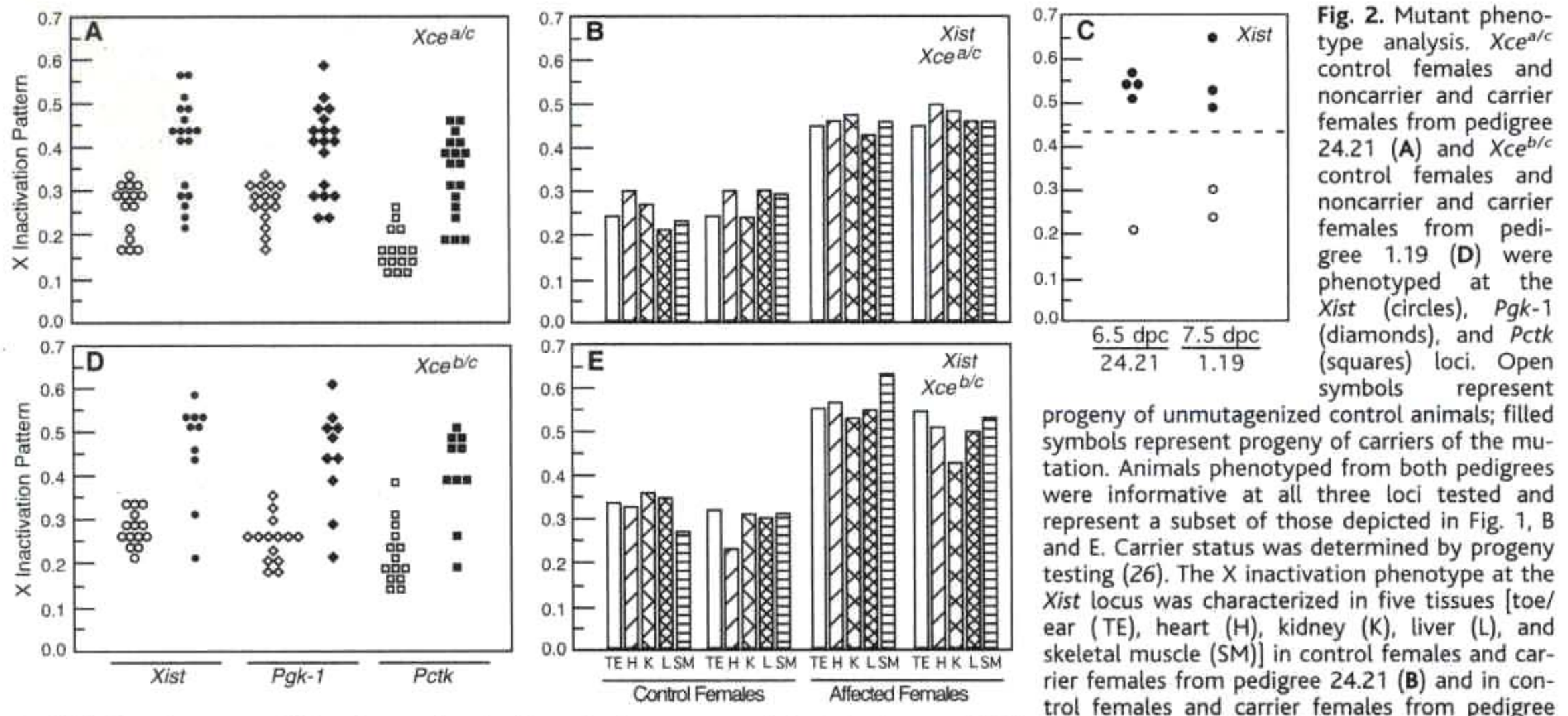

Fig. 2. Mutant phenotype analysis. $Xce^{a/c}$ control females and noncarrier and carrier females from pedigree 24.21 (**A**) and $Xce^{b/c}$ control females and noncarrier and carrier females from pedigree 1.19 (**D**) were phenotyped at the *Xist* (circles), *Pgk*-1 (diamonds), and *Pctk* (squares) loci. Open symbols represent progeny of unmutagenized control animals; filled symbols represent progeny of carriers of the mutation. Animals phenotyped from both pedigrees were informative at all three loci tested and represent a subset of those depicted in Fig. 1, B and E. Carrier status was determined by progeny testing (*26*). The X inactivation phenotype at the *Xist* locus was characterized in five tissues [toe/ear (TE), heart (H), kidney (K), liver (L), and skeletal muscle (SM)] in control females and carrier females from pedigree 24.21 (**B**) and in control females and carrier females from pedigree 1.19 (**E**). To minimize variability due to clonal cell populations, we sampled whole tissues. (**C**) X inactivation phenotype at the *Xist* locus in 6.5 days postcoitus (dpc) and 7.5 dpc control female embryos (open circles) and in 6.5 dpc 24.21 and 7.5 dpc 1.19 carrier embryos (closed circles). Carrier status of 24.21 embryos was established by genotyping at loci on chromosome 15 (*34*). Carrier status of 1.19 embryos was assigned on the basis of X inactivation patterns > 2 SD above the control mean of postnatal tissues (dashed line).

terns did not result from genetic background variability (*27*), consistent with previous studies (*22*). As further validation of the mutant phenotypes, we progeny tested unaffected female siblings in both pedigrees; as expected, their offspring demonstrated X inactivation patterns not significantly different from controls of the same cross ($P > 0.1$) (Fig. 1, B, C, E, and F).

Neither carrier males nor females exhibited obvious developmental defects, impaired fertility, or reduced segregation of the mutant phenotypes in either pedigree, which indicates specificity of the mutant phenotype to X inactivation. We characterized carrier mice for each mutation at three different X-linked loci: *Xist*, *Pctk*, and *Pgk-1* (*24*). The results of the assays were highly concordant for females tested in both pedigrees (Fig. 2, A and D), which indicates that the phenotypes reflect the chromosomal pattern of X inactivation and do not reflect, for example, simple locus-specific effects. We also characterized the X inactivation pattern in a variety of tissues representing the three embryonic lineages and determined that all tissues are similarly affected in carrier females from both pedigrees (Fig. 2, B and E).

Because X inactivation occurs early in embryonic development (*1*, *28*–*31*), these observations suggested that the mutations likely act on an early step in the X inactivation pathway. To address this directly, we assayed the X inactivation pattern in early embryos, after choice has occurred (*2*, *3*, *32*) but before any secondary cell selection might have taken place (*25*). Indeed, we detected the mutant phenotype in early embryos of both families (Fig. 2C), confirming that the mutations have a primary effect on X inactivation and clearly ruling out secondary cell selection as the mechanism responsible for the mutant phenotypes. Further, the mutation segregating in pedigree 24.21 induced the mutant phenotype when transferred to a different *Xce* heterozygous genotype, which confirms the effect of this mutation on X chromosome choice and rules out the possibility of a strain-specific oddity (*27*). Carrier females from both pedigrees exhibited appropriate imprinting of the well-characterized *H19* gene (*27*, *33*). Together, these data strongly indicate that the mutations detected in pedigrees 24.21 and 1.19 specifically affect an early step of the X inactivation pathway to result in primary X inactivation patterns that are significantly different from those predicted by their *Xce* genotypes.

To determine whether the mutations were X-linked, we examined segregation of the mutant phenotype through two categories of male siblings: those carrying either a wild-type or an ENU-treated X chromosome. If the mutation were X-linked, none of the males in the first category and all in the second should

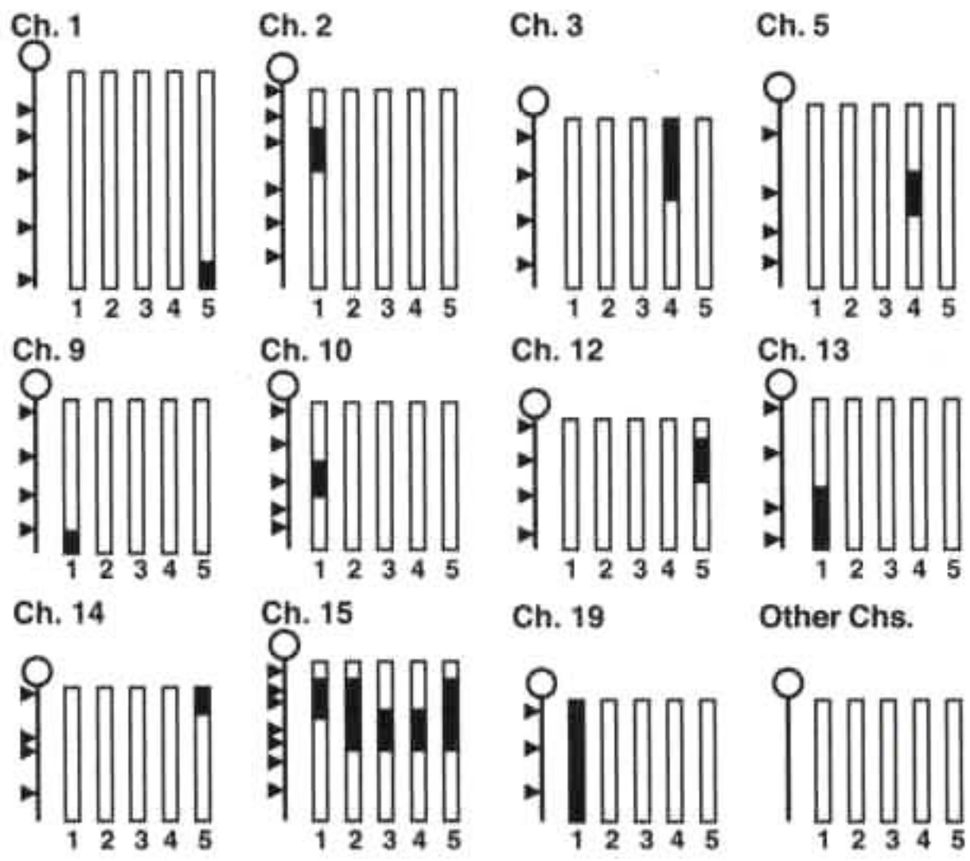

Fig. 3. Genome scan of pedigree 24.21 demonstrates linkage of the mutant phenotype to chromosome 15. Five affected G_4 and G_5 females were genotyped with microsatellite markers spaced evenly throughout the genome with a maximum spacing of 30 cM (*34*). The location of the markers is designated by arrowheads on the left of each chromosome. Genotypes for the five individual females are represented as vertical bars 1 through 5 for each chromosome. Unfilled regions of the bars represent wild-type genotypes (from the nonmutagenized parent); filled regions represent BALB/cByJ alleles inherited from the ENU-treated founder male. The probability that the ENU-treated alleles were inherited in the proximal region of chromosome 15 by chance is $P < 0.004$. Alleles from the ENU-treated male were not observed on chromosomes 4, 6, 7, 8, 11, 16, 17, and 18 (Other Chs.) (*27*) [fig. S1 (*35*)].

transmit the mutation to each of their daughters. On the other hand, if the mutation were autosomal, half the males in each category should transmit the phenotype to half their daughters. Indeed, about half the males in both categories in each family clearly transmitted the abnormal X inactivation pattern to a subset of their daughters (*27*), which indicates autosomal dominant modes of inheritance. Analysis of X-linked microsatellite markers in affected and unaffected family members in both pedigrees confirmed these observations (*27*). These data rule out X linkage in both families and are consistent with expectations of autosomal inheritance.

To localize the mutation in pedigree 24.21, we conducted a genome scan that took advantage of the genetic cross used to generate the pedigree. In this cross, we outcrossed the mutagenized G_0 BALB/cByJ founder male (*23*, *26*) and all subsequent generations to a tester strain carrying a *M. musculus castaneus* X chromosome (*22*, *23*). For the mapping analysis, we genotyped five affected and five unaffected distantly related females from the fourth (G_4) and fifth (G_5) generations with microsatellite markers evenly spaced across the genome with a maximum spacing of 30 centimorgans (cM) [Fig. 3 (*27*, *34*); fig. S1 (*35*)]. We observed alleles from the mutagenized BALB/cByJ founder male at the expected frequency, about 6.25 and 3.13% in G_4 and G_5 animals, respectively. The proximal half of chromosome 15 was the only region of the genome with significant linkage to the mutant phenotype ($P < 0.004$) [Fig. 3 (*34*); fig. S1 (*35*)]. This region does not contain any genes for factors known to be involved in any aspect of X inactivation or epigenetic silencing (including CTCF), which indicates that the mutation affects a specific factor in the X inactivation pathway. To determine whether the mutation in pedigree 1.19 involves the same locus, we genotyped chromosome 15 in affected animals from this pedigree (*27*); we observed no association between the mutant phenotype and chromosome 15. Although mapping of the 1.19 mutation to a specific location has been hindered by the lack of suitable informative markers that distinguish the strains used in this cross (*26*, *27*), these data indicate that the mutation segregating in the 1.19 pedigree involves an autosomal locus distinct from that mutated in the 24.21 pedigree.

These mutations, which we designate X-inactivation autosomal factors 1 and 2 (*Xiaf1* and *Xiaf2*), represent direct genetic evidence of autosomal factors in X inactivation. Functional and genetic studies of possible interactions between *Xiaf1* and *Xiaf2* and elements of the *Xic* (*16*–*19*), as well as further genetic mapping and positional cloning, will be required to elucidate the role of these autosomal factors in the X inactivation pathway.

References and Notes

1. M. F. Lyon, *Nature* **190**, 372 (1961).
2. P. Avner, E. Heard, *Nature Rev.* **2**, 59 (2001).
3. R. M. Boumil, J. T. Lee, *Hum. Mol. Genet.* **10**, 2225 (2001).
4. E. Heard, P. Clerc, P. Avner, *Annu. Rev. Genet.* **31**, 571 (1997).
5. C. J. Brown *et al.*, *Nature* **349**, 38 (1991).
6. G. D. Penny, G. F. Kay, S. A. Sheardown, S. Rastan, N. Brockdorff, *Nature* **379**, 131 (1996).
7. J. T. Lee, L. S. Davidow, D. Warshawsky, *Nature Genet.* **21**, 400 (1999).
8. N. Stavropoulos, N. Lu, J. T. Lee, *Proc. Natl. Acad. Sci. U.S.A.* **98**, 10232 (2001).
9. B. M. Cattanach, *Annu. Rev. Genet.* **9**, 1 (1975).
10. B. M. Cattanach, P. Johnston, *Hereditas* **94**, 5 (1981).
11. P. G. Johnston, B. M. Cattanach, *Genet. Res.* **37**, 151 (1981).
12. S. Rastan, *Genet. Res.* **40**, 139 (1982).
13. B. M. Cattanach, C. E. Williams, *Genet. Res.* **19**, 229 (1972).
14. B. M. Cattanach, C. Rasberry, *Mouse Genome* **92**, 114 (1994).
15. B. Courtier, E. Heard, P. Avner, *Proc. Natl. Acad. Sci. U.S.A.* **92**, 3531 (1995).
16. L. B. Russell, N. L. Cacheiro, *Basic Life Sci.* **12**, 393 (1978).
17. M. F. Lyon, *Nature New Biol.* **232**, 229 (1971).
18. S. Rastan, *J. Embryol. Exp. Morphol.* **78**, 1 (1983).
19. S. W. Brown, H. S. Chandra, *Proc. Natl. Acad. Sci. U.S.A.* **70**, 195 (1973).
20. W. Chao, K. D. Huynh, R. J. Spencer, L. S. Davidow, J. T. Lee, *Science* **295**, 345 (2002).
21. I. Percec, M. S. Bartolomei, *Science* **295**, 287 (2002).
22. R. M. Plenge, I. Percec, J. H. Nadeau, H. F. Willard, *Mamm. Genome* **11**, 405 (2000).
23. We conducted ENU mutagenesis on BALB/cByJ and B6CBAF1/J male mice (The Jackson Laboratory, Bar Harbor, ME) as described in (*36*). Mutagenized males and control unmutagenized males of the same genetic background were bred to tester mice containing a *M. musculus castaneus* (CAST/Ei) X chromosome on a 129X1/SvJ background (*22*). The tester strain of mice has been maintained by brother-sister mating for 7 to 10 generations. The X inactivation phenotype was first established in wild-type control females to provide a statistical basis for screening the female offspring of ENU-treated males. The X inactivation pattern in 66 wild-type $Xce^{a/c}$ females was normally distributed with a mean of 0.23 and a SD of 0.08. The X inactivation pattern in 89 wild-type $Xce^{b/c}$ females also was normally distributed with a mean of 0.28 and a SD of 0.1. Both distributions were consistent with previous analyses (*22*).
24. We conducted the *Pctk* assay on control and G_1 animals as described in (*22*). We analyzed subsequent generations with LightCycler (Roche) real time polymerase chain reaction (PCR) assays using fluorescence resonance energy transfer (FRET) probe technology (Roche). RNA samples were obtained from whole adult and embryonic tissues essentially as described in (*22*). About 0.75 μg of RNA was reverse transcribed in a 20-μl reaction mixture containing 10 mM dithiothreitol, 500 μM of each dNTP, 1× first strand buffer (GibcoBRL), 25 ng of random primers, 200 units of M-MLV reverse transcriptase (GibcoBRL), and 20 units of RNaseOUT ribonuclease inhibitor (GibcoBRL) by incubating for 10 min at room temperature, 60 min at 37°C, and 10 min at 95°C. For the *Xist* assay, the polymorphism is at nucleotide +323, between CAST/Ei (T) and other inbred strains (A). The primers Xist-F 5′-CTCGTTTCCCGTGGATGTG-3′ and Xist-R 5′-CCGATGGGCTAAGGAGAAG-3′ amplify a product of 490 base pairs (bp). FRET hybridization probes were designed to the non-CAST/Ei amplicon: XistM 5′-ATTCTTGCCCATCGGGGCCAC-3′ and XistA 5′-GATACCTGTGTGTCCTCCCCGCC-3′. For the *Pctk* assay, the polymorphism is at nucleotide +1752, between CAST/Ei (G) and other inbred strains (A) (*37*). The primers Pctk-F 5′-CAGTTTGAGGGTCGCAATCG-3′ and Pctk-R 5′-TGGCTCAGGCAGGTAAGCAGG-3′ amplified a product of 337 bp. FRET hybridization probes were designed to the non-CAST/Ei amplicon: PctkM 5′-GAGGTACAGCTACAAAAGGAGGC-3′ and PctkA 5′-AACATTCGGTCCACTTCTATGCCTGAC-3′. For the *Pgk-1* assay, the polymorphism is at nucleotide +163, between CAST/Ei (T) and other inbred strains (C). The primers PgkF 5′-CGTGATGAGGGTGGACTTCAAC-3′ and Pgk-R 5′-TAGTTTGGACAGTGAGGCTCGG-3′ amplified a product of 415 bp. FRET hybridization probes were designed to the non-CAST/Ei amplicon: PgkM 5′-CTGTTCCAAGCATCAAATTCTGCT-3′ and PgkA 5′-GGACAATGGAGCCAACTCCGTTGT-3′. Specific cycling conditions for the LightCycler assays are available upon request. The X inactivation pattern for the *Pctk* and *Pgk-1* assays was calculated as the expression of the *M. musculus domesticus* allele relative to the combined expression of both alleles (*22*). For the *Xist* assay, because *Xist* is expressed only from the inactive X, the X inactivation pattern was calculated as the percent expression of the CAST/Ei allele relative to the total expression. Thus, for all assays, the pattern represents the proportion of cells in which the inbred strain-derived X chromosome is the X_a. *P* values for the phenotype analysis were calculated with an unpaired Student's *t* test.
25. A. McMahon, M. Monk, *Genet. Res.* **41**, 69 (1983).
26. Pedigree 24.21 was generated from the daughter of a mutagenized BALB/cByJ male and segregates the $Xce^{a/c}$ genotype. Pedigree 1.19 was generated from the daughter of a mutagenized B6CBAF1/J male and segregates the $Xce^{b/c}$ genotype. In both pedigrees, carrier status was defined on the basis of Bayesian statistics by transmission of the affected phenotype (an X inactivation pattern > 2 SD above the mean) to a minimum of two female offspring. Given the distributions in Fig. 1, A and D, the likelihood of such an event occurring by chance is <0.01.
27. I. Percec, unpublished data.
28. M. N. Nesbitt, *Dev. Biol.* **26**, 252 (1971).
29. N. Takagi, *Exp. Cell Res.* **86**, 127 (1974).
30. M. Monk, M. I. Harper, *Nature* **281**, 311 (1979).
31. S. S. Tan, E. A. Williams, P. P. Tam, *Nature Genet.* **3**, 170 (1993).
32. S. Rastan, *J. Embryol. Exp. Morphol.* **71**, 11 (1982).
33. M. S. Bartolomei, S. Zemel, S. M. Tilghman, *Nature* **351**, 153 (1991).
34. We extracted DNA from tail and embryonic tissues by incubating overnight at 55°C in lysis buffer [50 mM KCl, 1.5 mM $MgCl_2$, 10 mM Tris-HCl (pH 8.5), 0.01% gelatin, 0.45% Igepal CA-630, 0.45% Tween 20, 0.6 mg of proteinase K per ml] followed by incubation at 95°C for 10 min. We used 1 μl of the supernatant for genotyping PCR. Genotyping of the X chromosome employed the *DXMit53*, *DXMit141*, *DXMit22*, *DXMit18*, and *DXMit249* markers. Genotyping of the autosomes employed 85 microsatellite markers that distinguish strains BALB/cByJ from CAST/Ei and 129X1/SvJ. For chromosome 15, the markers used were *D15Mit13*, *D15Mit136*, *D15Mit6*, *D15Mit101*, *D15Mit3*, *D15Mit34*, and *D15Mit16*. For amplification, 100 ng of DNA and 0.5 μM of each primer were added to a Ready-To-Go PCR bead. Denaturation at 95°C for 2 min was followed by 35 cycles of amplification at 95°C for 15 s, 55°C for 10 s, and 72°C for 20 s. The *P* value for the genome scan was calculated as the probability of random segregation of the mutant alleles to the animals tested.
35. Supplemental material (fig. S1) is available on *Science* Online at www.sciencemag.org/cgi/content/full/296/5570/1136/DC1.
36. J. S. Weber, A. Salinger, M. J. Justice, *Genesis* **26**, 230 (2000).
37. L. Carrel *et al.*, *Hum. Mol. Genet.* **5**, 391 (1996).

38. Supported by NIH grant GM45441 (H.F.W.) and the Howard Hughes Medical Institute (M.S.B.). I.P. was supported by an NIH Radiation Biology predoctoral training grant. We thank M. Justice and J. Amos-Landgraf for helpful assistance with mutagenesis; W. Ewens, D. Beier, and R. Spielman for statistical advice; and C. Krapp and K. Olszens for animal husbandry and dissections.

22 January 2002; accepted 3 April 2002